



Construction of miRNAs and Gene Expression Profiles Associated with Ischemic Cardiomyopathy: Bioinformatics Analysis

Phong Son Dinh^{1,2}, Jun-Hua Peng^{1,3}, ChauMy Thanh Tran², Thanh Loan Tran^{1,4}, Shang-Ling Pan^{1,3*}

¹Departments of Pathophysiology, Guangxi Medical University, Guangxi, China; ²Department of Medicine and Pharmacy, Duy Tan University, Da Nang, Vietnam; ³Department of Medicine, GuSSangxi Medical University, Guangxi, China; ⁴Department of Immunology and Pathophysiology, Hue University of Medicine and Pharmacy, Hue University, Vietnam

ABSTRACT

Objective: Ischemic Cardiomyopathy (ICM) has ranked as the most common cause morbidity and mortality in the elderly over the past decades. One of the most important reasons for this is that its exact underlying mechanism remains poorly understood.

Method: Five datasets were downloaded from the GEO database. Differential Gene Expression (DGE) was identified by the R RobustRankAggreg package. Differential miRNA expression was evaluated by the Limma package. Gene potential functions were then determined by the clusterProfiler database. The miRNA-DGE regulatory network was predicted by cyTargetLinker. Then, a protein-protein interaction network was constructed by STRING tool, MCODE, and BiNGO tool.

Results: 91 miRNAs and 274 potential genes were identified. Of these, *COL1A1*, *IGF1* and *CCND1* were found to be involved in many signaling pathways; and miR-9-5p was found to play critical roles in ICM.

Conclusion: Our study has unraveled the potential key genes and miRNAs as well as the possible underlying molecular pathogenesis of ICM, which is a crucial step leading to a new avenue for the early intervention of this disorder.

Keywords: Ischemic cardiomyopathy; Heart failure; MiRNAs; mRNA; Network; Bioinformatics

INTRODUCTION

Cardiomyopathies are disorders in which the myocardium is structurally and functionally abnormal and may lead to Heart Failure (HF); The etiology can be divided into non-ischemic and ischemic causes. The former is designated cardiomyopathy independent of ischemic events, and can be caused by hypertension, valvular pathologies, toxins, or inheritance. Ischemic Cardiomyopathy (ICM) is defined as systolic dysfunction of the Left Ventricle (LV) due to Myocardial Infarction (MI), or >75% occlusion of a major coronary artery [1]. Extensive myocardial ischemia may result in acute and severe infarction of the ventricular wall and resultant HF with high mortality; whereas moderate and mild ventricular ischemia with less stenosis of the coronary artery may lead to chronic left

ventricle impairment, typically presenting as myocardial stunning, hibernation and ventricular remodeling [2,3]. These manifestations have been ascribed to a series of pathological processes-inflammation, metabolic dysfunction, fibrosis and scarring of myocardial cells or extracellular matrix [4,5], resulting in progressive degradation of cardiac contractility, ventricular dilatation, and eventually chronic heart failure.

Once initiated, a chronic pathology is progressive and irreversible. Cardiologists attempt to slow the progression of chronically ICM-derived heart failure. The limited progress to date suggests that the research directions and identified signaling pathways-including inflammatory mediators (e.g., cytokines, chemokines) profibrotic and apoptotic factors (e.g., transforming

Correspondence to: Shang-Ling Pan, Departments of Pathophysiology, Guangxi Medical University, Guangxi, China; E-mail: slpan@gxmu.edu.cn

Received: 12-Oct-2022, Manuscript No. GJBAHS-22-18314; **Editor assigned:** 17-Oct-2022, PreQC No. GJBAHS-22-18314 (PQ); **Reviewed:** 31-Oct-2022, QC No. GJBAHS-22-18314; **Revised:** 13-Feb-2023, Manuscript No. GJBAHS-22-18314 (R); **Published:** 20-Feb-2023, DOI: 10.35248/2319-5584.23.12.162

Citation: Dinh PS, Peng JH, Tran CMT, Tran TL, Pan SL (2023) Construction of MiRNAs and Gene Expression Profiles Associated With Ischemic Cardiomyopathy: Bioinformatics Analysis. Glob J Agric Health Sci. 12:162.

Copyright: © 2023 Dinh PS, et al. This is an open-access article distributed under the terms of the Creative Commons Attribution License, which permits unrestricted use, distribution, and reproduction in any medium, provided the original author and source are credited.

growth factor β) and remodeling associated component matrix metalloproteinases are not the sole contributors to ICM [6,7].

MicroRNAs (miRNAs) are highly conserved non-coding RNAs of approximately 22 nucleotides and are widely expressed in eukaryotes, miRNAs regulate the expression of target genes at the post-transcriptional level by binding to their 3'-untranslated regions [8,9]. Many miRNAs are implicated in the development of ICM [7-11]. Therefore, miRNAs are key players in the pathogenesis of ICM.

Based on miRNAs in public databases and bioinformatics, we constructed an interactive network between ICM associated miRNAs and related genes and signaling pathways, including genes linked to early diagnosis and prognosis of ICM.

MATERIALS AND METHODS

Data acquisition and rank aggregation methods

ICM Differentially Expressed Gene (DEG) datasets based on human heart tissue; more than three left ventricular samples from patients and healthy controls, and evaluation of miRNA/mRNA expression in ICM were retrieved from the public database Gene Expression Omnibus (GEO) (Figure 1). The gene expression datasets used were GSE16499 (GPL5175), GSE48166 (GPL9115), GSE46224 (GPL11154), GSE57338 (GPL11532), and GSE76701 (GPL570) [12-16].

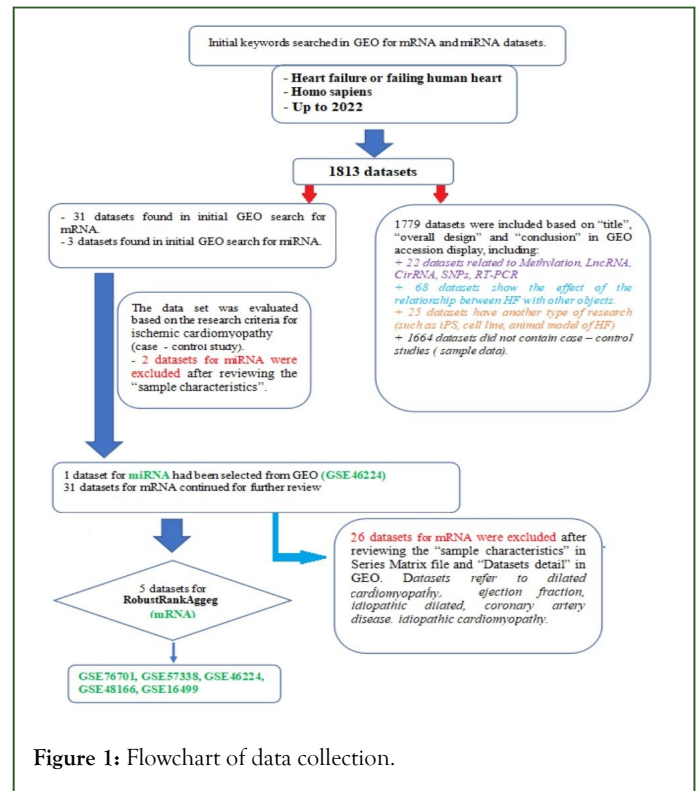


Figure 1: Flowchart of data collection.

A total of 315 samples (178 ICM and 137 control samples) met the criteria for analysis. Eight ICM and eight control samples from GSE46224 (GPL11154) were subjected to differential miRNA expression analysis (Table 1). The GSE ID, high-throughput data, and characteristics of the control and ICM groups were collected in a series matrix file and analyzed by R v. 3.6.2.

Table 1: Databases used in this study.

GEO accession number	Subjects		Platform	
	control	ICM		
mRNA	GSE76701	4	4	Affymetrix human genome U133 plus 2.0 array
	GSE57338	95	136	Affymetrix human gene 1.1 ST array
	GSE46224	8	8	Illumina hiSeq 2000 (homo sapiens)
	GSE48166	15	15	Illumina genome analyzer II (Homo sapiens)
	GSE16499	15	15	Affymetrix human exon 1.0 ST array
miRNA	GSE46224	8	8	Illumina hiSeq 2000 (Homo sapiens)

R v.3.6.2, Bioconductor and linear model with datasets analysis (Limma) software were used to conduct differential miRNA expression and DEG analyses [17,18]. P values were corrected using the false discovery rate (FDR) correction toolkit in R v. 3.6.2 software. A p value <0.05 and FDR <0.05 for GSE (fold change >0.5) were regarded as indicative of a significant difference. DEGs common to more than one gene expression dataset were identified and visualized using the RobustRankAggreg package in R [19].

Gene Ontology (GO) and Kyoto Encyclopedia of Genes and Genomes (KEGG) enrichment analyses

To assess the functions of Differentially Expressed Genes (DEGs) in ICM, the clusterProfiler package v.14.3 was used for GO and signaling pathway analyses. A p<0.05 was used as the cut-off to determine significant enrichment [20].

Construction of the miRNA-mRNA regulatory network and module analysis based on the Protein-Protein Interaction (PPI) network.

The KEGG pathway and miRNA analysis results were transferred to Cytoscape v.3.6.1 and used to construct a network. The regulatory network was predicted by cyTargetLinker using the targetsan-hsa-7, miRTarBase-hsa-7,

and miRBase-hsa-v2.1databases [21]. A miRNA-potential gene network was constructed using a gene regulatory subnetwork. The search tool for the retrieval of interacting genes/proteins (STRING) database was used to construct a PPI network [22]. Modules comprising genes of similar biological functions were analyzed using the Mcode package in Cytoscape software (adjusted p<0.05). A K-core ≥ 2 , node score cutoff =0.2, degree cutoff ≥ 2 and MCODE score ≥ 3 were the cutoff values for module analysis. Functionally associated genes in the modules were classified using the BiNGO tool.

RESULTS

Identification of differentially expressed genes and miRNAs in ICM

The DEG analyses revealed 179 up-regulated and 95 down-regulated genes in left ventricle samples (Table 2). Additionally, there were 91 differentially expressed miRNAs in ICM, comprising 45 up-regulated and 46 down-regulated miRNAs (Table 3). The top 10 up and down-regulated genes and miRNAs are listed in Tables 4 and 5, respectively.

Table 2: The DGE analyses revealed 179 up-regulated and 95 down-regulated genes from 5 genetic databases.

Up regulated	log2FC	p value	Down regulated	log2FC	p value
<i>HBB</i>	2.354376	1.59E-14	<i>SERPINA3</i>	-1.98731	1.63E-16
<i>NPPA</i>	2.34081	7.78E-13	<i>MYH6</i>	-1.82385	1.24E-15
<i>NPPB</i>	1.789251	8.00E-10	<i>FCN3</i>	-1.4565	8.55E-14
<i>SFRP4</i>	1.462998	5.68E-10	<i>CD163</i>	-1.26507	6.30E-11
<i>HBA1</i>	1.395612	9.99E-08	<i>CYP4B1</i>	-1.20673	1.21E-07
<i>EIF1AY</i>	1.380697	8.82E-06	<i>VSIG4</i>	-1.18622	8.79E-10
<i>MXRA5</i>	1.351716	1.89E-12	<i>METTL7B</i>	-1.10309	2.73E-12
<i>ASPN</i>	1.350178	4.78E-11	<i>PLA2G2A</i>	-1.05118	3.94E-08
<i>FMOD</i>	1.323499	7.76E-11	<i>F13A1</i>	-0.98689	2.21E-08
<i>HBA2</i>	1.31982	3.15E-07	<i>ANKRD2</i>	-0.96234	3.86E-09
<i>LUM</i>	1.266873	8.17E-12	<i>LYVE1</i>	-0.95738	1.52E-08

<i>THBS4</i>	1.101911	8.24E-11	<i>IL1RL1</i>	-0.87654	3.21E-07
<i>MFAP4</i>	1.098181	8.07E-10	<i>HMGCS2</i>	-0.82633	2.74E-07
<i>AEBP1</i>	1.081074	2.35E-08	<i>S100A9</i>	-0.80122	3.92E-08
<i>POSTN</i>	1.053017	1.14E-08	<i>RNASE2</i>	-0.79677	2.09E-07
<i>LTBP2</i>	1.044266	6.77E-08	<i>MYOT</i>	-0.79395	1.62E-06
<i>RPS4Y1</i>	1.037478	0.000589	<i>NPTX2</i>	-0.77126	2.39E-06
<i>EGR1</i>	1.032011	1.62E-06	<i>FAM46B</i>	-0.76809	2.01E-06
<i>COL14A1</i>	1.016907	4.86E-10	<i>BLM</i>	-0.73559	5.40E-05
<i>OGN</i>	1.013501	3.86E-09	<i>GRB14</i>	-0.72104	1.50E-06
<i>UCHL1</i>	1.005952	3.53E-09	<i>DHRS7C</i>	-0.72077	5.64E-06
<i>CHRD1</i>	0.999873	5.07E-08	<i>FKBP5</i>	-0.7076	2.69E-06
<i>SMOC2</i>	0.986773	6.06E-09	<i>CA14</i>	-0.69449	3.60E-07
<i>PENK</i>	0.984512	1.16E-06	<i>AQP4</i>	-0.69229	2.04E-08
<i>FRZB</i>	0.980063	1.06E-08	<i>FCGBP</i>	-0.66716	1.03E-08
<i>ISLR</i>	0.927885	3.04E-11	<i>SLCO4A1</i>	-0.66423	0.000163
<i>PI16</i>	0.923988	7.64E-10	<i>TIMP4</i>	-0.65999	1.62E-05
<i>USP9Y</i>	0.900058	4.26E-05	<i>CSDC2</i>	-0.65778	2.14E-05
<i>CTGF</i>	0.88894	1.75E-06	<i>XIST</i>	-0.65558	0.0021
<i>PHLDA1</i>	0.865894	8.71E-10	<i>CD14</i>	-0.65484	3.26E-06
<i>KDM5D</i>	0.854993	0.000875	<i>TUBA3D</i>	-0.6405	0.000238
<i>BEX1</i>	0.844901	2.74E-07	<i>FCER1G</i>	-0.63578	2.07E-05
<i>PTN</i>	0.835055	1.62E-06	<i>MID1IP1</i>	-0.63459	9.84E-09
<i>COL1A1</i>	0.818173	4.62E-07	<i>ADAMTS15</i>	-0.62782	7.09E-06
<i>OMD</i>	0.785744	2.16E-07	<i>GFPT2</i>	-0.62641	0.000158
<i>DPT</i>	0.762057	3.15E-08	<i>MGST1</i>	-0.61413	0.00022

TNNT1	0.752141	2.58E-08	SGPP2	-0.61057	7.35E-06
COL1A2	0.742222	4.64E-06	AOX1	-0.59946	0.000238
SCN2B	0.729555	1.15E-07	ART3	-0.59753	0.000181
STAT4	0.723911	5.43E-05	PLIN2	-0.5925	2.53E-06
SULF1	0.720519	2.83E-07	CHST9	-0.58918	0.00017
COLQ	0.719308	2.00E-08	C1orf162	-0.58115	1.14E-05
CCDC80	0.714976	9.62E-05	ANXA3	-0.57728	0.000535
COMP	0.713881	0.004499	KCND3	-0.5758	4.82E-05
PRELP	0.712364	7.20E-07	MRC1	-0.57013	0.007844
NAP1L3	0.70466	5.13E-05	HMOX2	-0.57011	7.49E-05
CRYM	0.69382	5.52E-08	ALOX5AP	-0.56837	8.08E-06
FBLN1	0.69134	2.09E-07	HOGA1	-0.56732	0.005146
SDSL	0.689707	2.39E-08	CHDH	-0.56678	2.87E-06
ECM2	0.688057	7.77E-08	KIAA0040	-0.56298	1.16E-05
HTRA1	0.680078	1.85E-08	CADPS2	-0.56278	0.000102
ITIH5	0.679739	2.04E-07	MPP3	-0.55754	8.91E-07
EXT1	0.661279	2.30E-08	GNMT	-0.5568	0.003539
FND1	0.660297	0.000186	SLC19A2	-0.55542	0.00523
OGDHL	0.655201	1.47E-06	CCR1	-0.55433	0.001116
CFH	0.654649	4.14E-06	SIPR3	-0.55102	0.000794
EDNRA	0.646022	9.93E-08	GALNT15	-0.55096	0.006851
DPYSL3	0.644603	4.07E-09	LCN6	-0.54502	0.000382
ABCG2	0.638882	2.19E-06	PPP1R1A	-0.54235	1.61E-05
WNT9A	0.636478	2.06E-05	EIF4EBP1	-0.54088	0.002899
SCUBE2	0.62144	1.18E-06	SHISA3	-0.53843	0.000773
EGR2	0.619645	0.001343	CYBB	-0.53667	0.005104
PLCE1	0.61819	6.36E-06	CNTN3	-0.53361	0.010493
RASL11B	0.613471	3.54E-08	PTDSS1	-0.53313	9.43E-05
C16orf89	0.610304	1.36E-07	CPAMD8	-0.52937	0.000175
FREM1	0.609033	9.26E-07	CIQC	-0.52718	6.41E-05
HSPA2	0.606243	2.93E-06	LPCAT3	-0.527	1.53E-05

<i>CRISPLD1</i>	0.604811	0.000359	<i>CD300LG</i>	-0.52532	0.000224
<i>ITGBL1</i>	0.600457	4.44E-05	<i>EDNRB</i>	-0.52203	0.000242
<i>PROM1</i>	0.59972	0.00196	<i>PPL</i>	-0.52165	0.003945
<i>HSPB6</i>	0.599308	0.002119	<i>LAPTM5</i>	-0.52045	0.000561
<i>NRK</i>	0.598138	0.000275	<i>LCN10</i>	-0.51995	8.34E-05
<i>IFI44L</i>	0.598121	7.33E-05	<i>MT1X</i>	-0.51913	2.93E-05
<i>TSPAN9</i>	0.595701	5.89E-08	<i>SLA</i>	-0.51847	0.000882
<i>ENO2</i>	0.593566	1.50E-05	<i>NQO1</i>	-0.51689	0.004923
<i>IFIT3</i>	0.59088	0.000128	<i>AASS</i>	-0.51477	0.000676
<i>PLVAP</i>	0.590604	0.00347	<i>AGXT2L1</i>	-0.51433	4.44E-05
<i>APOA1</i>	0.589269	0.000589	<i>TUBA3E</i>	-0.51316	0.000946
<i>SLC16A9</i>	0.588328	9.37E-06	<i>C3AR1</i>	-0.51301	0.000324
<i>IRX6</i>	0.58811	0.004721	<i>C1QTNF1</i>	-0.50948	0.000155
<i>CH25H</i>	0.584188	0.000786	<i>MT1A</i>	-0.50908	2.76E-05
<i>ARHGAP1</i>	0.583454	6.89E-06	<i>C1orf105</i>	-0.50819	0.000148
<i>DDX3Y</i>	0.583137	0.000114	<i>FAM58A</i>	-0.50795	2.72E-06
<i>TLL2</i>	0.581768	0.000648	<i>CD38</i>	-0.50743	8.51E-05
<i>RGS4</i>	0.580226	1.45E-05	<i>CHL1</i>	-0.50732	4.74E-07
<i>EPHA3</i>	0.578333	6.44E-06	<i>CHRD2</i>	-0.50574	3.91E-06
<i>SNCA</i>	0.578109	0.000662	<i>S100A8</i>	-0.5052	0.000337
<i>ANTXR1</i>	0.573179	5.30E-07	<i>TLR2</i>	-0.5047	6.59E-06
<i>CPXM2</i>	0.573154	2.84E-05	<i>ST6GALNAC3</i>	-0.50451	0.003895
<i>TMEM71</i>	0.571884	3.80E-06	<i>C1QB</i>	-0.50426	7.66E-05
<i>IFI6</i>	0.570762	0.000388	<i>ITGAM</i>	-0.50382	0.044109
<i>SYTL2</i>	0.570436	0.001321	<i>CHAC2</i>	-0.50322	1.22E-05
<i>CCND1</i>	0.5665	3.52E-05	<i>C19orf33</i>	-0.50255	9.66E-06
<i>IGSF10</i>	0.566376	4.38E-06	<i>F8</i>	-0.50207	2.77E-06
<i>COL3A1</i>	0.564112	0.000455	<i>CPM</i>	-0.50036	0.005924
<i>IFIT2</i>	0.562754	6.83E-05			
<i>PLAT</i>	0.562088	1.41E-05			
<i>BGN</i>	0.561579	8.87E-05			

<i>ARRDC3</i>	0.561354	4.11E-05
<i>KLHL13</i>	0.561187	3.14E-06
<i>PROS1</i>	0.56106	0.0001
<i>SFRP1</i>	0.559602	0.000316
<i>MYH10</i>	0.559049	1.15E-06
<i>CA3</i>	0.556052	0.001758
<i>SOD3</i>	0.555893	0.001148
<i>MXRA8</i>	0.55455	0.001816
<i>APLNR</i>	0.554224	0.009911
<i>LEPREL1</i>	0.550828	1.19E-05
<i>LTBP4</i>	0.550778	1.02E-06
<i>FZD7</i>	0.54696	0.000117
<i>PTGFRN</i>	0.546192	2.93E-06
<i>CCDC3</i>	0.545999	3.49E-06
<i>EPHX2</i>	0.54456	0.000438
<i>MDK</i>	0.544266	5.52E-06
<i>OLFML1</i>	0.543044	0.000561
<i>NT5E</i>	0.542511	0.000683
<i>F2R</i>	0.541087	1.29E-05
<i>PLEKHH2</i>	0.540168	0.000648
<i>COL12A1</i>	0.537753	1.04E-05
<i>JAK2</i>	0.537614	7.80E-07
<i>ANKRD34C</i>	0.536623	0.013917
<i>FAP</i>	0.53648	7.17E-05
<i>PDE5A</i>	0.535575	0.000147
<i>LTBP3</i>	0.534715	1.77E-06
<i>MATN2</i>	0.534396	1.44E-06
<i>APLP1</i>	0.534231	6.19E-05
<i>FIBIN</i>	0.534106	4.11E-05
<i>C10orf71</i>	0.533052	1.50E-06
<i>PDGFD</i>	0.532947	5.27E-06

<i>USP11</i>	0.53191	1.37E-05
<i>DIO2</i>	0.531729	0.00131
<i>MYO1D</i>	0.531609	0.000333
<i>CILP</i>	0.53014	0.003134
<i>LMOD2</i>	0.529885	0.001444
<i>HIST1H2AK</i>	0.528932	2.67E-06
<i>IER2</i>	0.528367	0.009569
<i>TNFRSF11B</i>	0.526274	0.003968
<i>MSS51</i>	0.52608	0.000337
<i>ANO1</i>	0.52558	1.53E-06
<i>COL8A1</i>	0.524591	0.000102
<i>EGLN3</i>	0.524533	0.000175
<i>SLN</i>	0.524325	0.004737
<i>IGFBP5</i>	0.524251	3.63E-05
<i>COL16A1</i>	0.523228	0.000101
<i>MYOC</i>	0.522538	0.005314
<i>PIK3IP1</i>	0.521146	2.57E-06
<i>PODN</i>	0.521111	2.14E-05
<i>KCNN3</i>	0.521108	0.000105
<i>ENPP2</i>	0.520779	0.000985
<i>PPDPF</i>	0.520519	0.000635
<i>GSTM5</i>	0.519283	0.000337
<i>MRC2</i>	0.519052	1.83E-06
<i>MLLT11</i>	0.518545	0.001216
<i>FGF1</i>	0.517916	1.55E-07
<i>THY1</i>	0.51708	0.015446
<i>CCDC113</i>	0.516188	0.000622
<i>SERPINI1</i>	0.515853	9.62E-05
<i>ABI3BP</i>	0.515456	9.24E-06
<i>ZMYND17</i>	0.514868	0.000443
<i>MAFK</i>	0.513922	0.003456

<i>CXCL14</i>	0.51383	0.001258
<i>PCOLCE2</i>	0.513638	0.001013
<i>COL21A1</i>	0.513236	1.59E-05
<i>SCRN1</i>	0.510007	0.000841
<i>ODC1</i>	0.509858	0.002936
<i>MNS1</i>	0.509554	0.000128
<i>TRIL</i>	0.509317	0.006618
<i>XG</i>	0.508436	4.61E-05
<i>CTSK</i>	0.508329	0.000121
<i>C1QTNF7</i>	0.507466	1.33E-05
<i>SNAP47</i>	0.506251	5.34E-06
<i>OAS1</i>	0.506243	0.000107
<i>GLT8D2</i>	0.506034	3.74E-06
<i>PLXDC2</i>	0.505973	0.000376
<i>SVEP1</i>	0.505702	0.000299
<i>THBS3</i>	0.504814	1.48E-05
<i>SERPINE2</i>	0.504807	0.033515
<i>IGF1</i>	0.50418	0.000604
<i>BOC</i>	0.503075	5.34E-06

Table 3: The differentially expressed miRNAs analyses revealed 45 up-regulated and 46 down-regulated miRNAs from GSE46224.

Up-regulated miRNA	log2FC	P value	Down-regulated miRNA	log2FC	P value
hsa-miR-144-3p	4.606894	0.001406	hsa-miR-221-5p	-2.6281	0.000131
hsa-miR-144-5p	4.342799	0.000127	hsa-miR-378b	-2.42053	0.045604
hsa-miR-182-5p	3.965608	7.46E-05	hsa-miR-4797-3p	-1.84247	0.024277
hsa-miR-451a	3.910478	0.0002	hsa-miR-9-5p	-1.77943	0.002412
hsa-miR-183-5p	3.782411	0.001284	hsa-miR-675-5p	-1.77241	0.002454
hsa-miR-184	2.666112	0.002998	hsa-miR-519c-3p	-1.65407	0.002811
hsa-miR-129-5p	2.327642	0.002222	hsa-miR-222-3p	-1.60432	1.17E-05

hsa-miR-4508	2.214633	0.004026	hsa-miR-520c-3p	-1.58706	0.024758
hsa-miR-34c-5p	2.160532	0.00038	hsa-miR-221-3p	-1.57555	2.94E-06
hsa-miR-96-5p	2.112541	0.033934	hsa-miR-378f	-1.54865	0.005427
hsa-miR-1246	2.007445	0.012235	hsa-miR-138-5p	-1.39156	0.049468
hsa-miR-4800-3p	1.896722	0.021801	hsa-miR-4441	-1.3709	0.04521
hsa-miR-190b	1.742823	0.01474	hsa-miR-1303	-1.36701	0.015669
hsa-miR-34c-3p	1.509602	0.000921	hsa-miR-548ao-3p	-1.36052	0.008756
hsa-miR-4492	1.375878	0.025098	hsa-miR-3679-5p	-1.3254	0.03725
hsa-miR-301b	1.331442	0.007796	hsa-miR-483-5p	-1.31768	0.003427
hsa-miR-155-5p	1.305902	0.004332	hsa-miR-1301	-1.27307	0.028351
hsa-miR-545-5p	1.26616	0.018262	hsa-miR-378i	-1.26763	0.006838
hsa-miR-5002-5p	1.207722	0.01083	hsa-miR-1323	-1.19812	0.02686
hsa-miR-3614-5p	1.189791	0.044558	hsa-miR-1254	-1.17484	0.004867
hsa-miR-3938	1.174843	0.004867	hsa-miR-378g	-1.08558	0.011694
hsa-miR-141-3p	1.165777	0.034331	hsa-miR-1306-3p	-1.05945	0.041574
hsa-miR-3688-3p	1.155039	0.038069	hsa-miR-20a-5p	-1.05769	0.00161
hsa-miR-708-5p	1.134239	0.005551	hsa-miR-302a-3p	-1.05233	0.013938
hsa-miR-542-3p	1.132806	0.046154	hsa-miR-362-5p	-0.99887	0.000989
hsa-miR-34b-5p	1.105441	0.038479	hsa-miR-150-5p	-0.99762	0.00265
hsa-miR-301a-5p	1.104563	0.032681	hsa-miR-1197	-0.93648	0.019612
hsa-miR-4707-3p	1.094361	0.04481	hsa-miR-490-5p	-0.91371	0.005685
hsa-miR-4732-3p	1.082722	0.02607	hsa-miR-422a	-0.90036	0.023588
hsa-miR-125b-1-3p	1.077469	0.022832	hsa-miR-4682	-0.89624	0.047849
hsa-miR-548h-3p	1.040241	0.024013	hsa-miR-17-5p	-0.88517	0.001473
hsa-miR-1285-5p	1.028602	0.025828	hsa-miR-429	-0.8846	0.020118
hsa-miR-320b	1.004797	0.002306	hsa-miR-548l	-0.8846	0.020118
hsa-miR-34b-3p	0.936482	0.030232	hsa-miR-302d-3p	-0.85135	0.02825
hsa-miR-493-3p	0.910269	0.025234	hsa-miR-486-5p	-0.84345	0.012492
hsa-miR-21-5p	0.896306	0.038306	hsa-miR-193a-5p	-0.8226	0.013911
hsa-miR-195-3p	0.894215	0.010732	hsa-miR-338-5p	-0.80922	0.030131
hsa-miR-130b-5p	0.86694	0.041394	hsa-miR-378e	-0.7788	0.046872

hsa-miR-708-3p	0.77362	0.033859	hsa-miR-378h	-0.76744	0.008128
hsa-miR-130b-3p	0.754336	0.034909	hsa-miR-665	-0.74033	0.029442
hsa-miR-339-5p	0.740642	0.041285	hsa-miR-29c-5p	-0.72317	0.020047
hsa-miR-106b-3p	0.730287	0.037179	hsa-miR-378a-3p	-0.70929	0.004223
hsa-miR-154-5p	0.717875	0.046722	hsa-miR-188-5p	-0.70922	0.038996
hsa-miR-769-5p	0.686929	0.023314	hsa-miR-499a-5p	-0.7	0.030848
hsa-miR-497-5p	0.51134	0.021255	hsa-miR-491-3p	-0.64498	0.026676
			hsa-miR-30c-5p	-0.53719	0.046957

Table 4: Top 10 up and down-regulated genes.

Up regulated	log2FC	P value	Down regulated	log2FC	P value
<i>HBB</i>	2.354376	1.59E-14	<i>SERPINA3</i>	-1.98731	1.63E-16
<i>NPPA</i>	2.34081	7.78E-13	<i>MYH6</i>	-1.82385	1.24E-15
<i>NPPB</i>	1.789251	8.00E-10	<i>FCN3</i>	-1.4565	8.55E-14
<i>SFRP4</i>	1.462998	5.68E-10	<i>CD163</i>	-1.26507	6.30E-11
<i>HBA1</i>	1.395612	9.99E-08	<i>CYP4B1</i>	-1.20673	1.21E-07
<i>EIF1AY</i>	1.380697	8.82E-06	<i>VSIG4</i>	-1.18622	8.79E-10
<i>MXRA5</i>	1.351716	1.89E-12	<i>METTL7B</i>	-1.10309	2.73E-12
<i>ASPN</i>	1.350178	4.78E-11	<i>PLA2G2A</i>	-1.05118	3.94E-08
<i>FMOD</i>	1.323499	7.76E-11	<i>F13A1</i>	-0.98689	2.21E-08
<i>HBA2</i>	1.31982	3.15E-07	<i>ANKRD2</i>	-0.96234	3.86E-09

Table 5: Top 10 up and downregulated miRNAs.

Upregulated miRNA	log2FC	p value	Downregulated miRNA	log2FC	p value
hsa-miR-144-3p	4.606894	0.001406	hsa-miR-221-5p	-2.6281	0.000131
hsa-miR-144-5p	4.342799	0.000127	hsa-miR-378b	-2.42053	0.045604
hsa-miR-182-5p	3.965608	7.46E-05	hsa-miR-4797-3p	-1.84247	0.024277
hsa-miR-451a	3.910478	0.0002	hsa-miR-9-5p	-1.77943	0.002412
hsa-miR-183-5p	3.782411	0.001284	hsa-miR-675-5p	-1.77241	0.002454
hsa-miR-184	2.666112	0.002998	hsa-miR-519c-3p	-1.65407	0.002811
hsa-miR-129-5p	2.327642	0.002222	hsa-miR-222-3p	-1.60432	1.17E-05

hsa-miR-4508	2.214633	0.004026	hsa-miR-520c-3p	-1.58706	0.024758
hsa-miR-34c-5p	2.160532	0.00038	hsa-miR-221-3p	-1.57555	2.94E-06
hsa-miR-96-5p	2.112541	0.033934	hsa-miR-378f	-1.54865	0.005427

GO and KEGG pathway enrichment analysis of DEGs

GO and pathway enrichment analyses revealed the up-regulated and down-regulated genes in ICM. Totals of 342 GO terms for up-regulated genes and 69 GO terms for down-regulated genes were identified. The GO terms for up-regulated genes indicated Molecular Function (MF) related pathways such as extracellular matrix structural constituent, collagen binding, Wnt-protein binding, proteoglycan binding, growth factor binding, glycosaminoglycan binding, and heparin binding. The GO terms for down-regulated genes indicated MF related pathways such as toll-like receptor binding, long-chain fatty acid binding, and lyase activity. The GO terms of associated genes were ranked by their adjusted p values ($p < 0.05$; adjusted $p < 0.05$) (Figure 2).

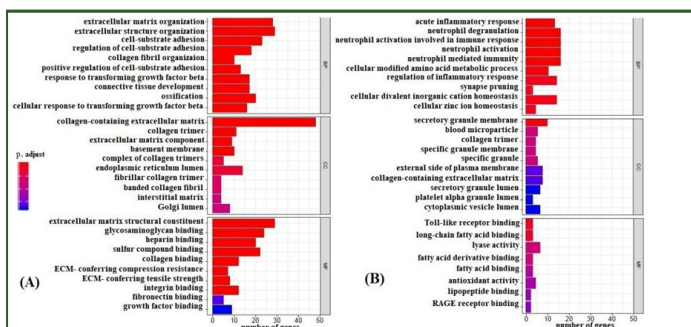


Figure 2: GO enrichment analysis of DEGs using the clusterProfiler package. (A) GO analysis of the top 10 upregulated DEGs in ICM (B) GO analysis of the top 10 downregulated DEGs in ICM. BP, biological process; CC, cellular component; MF, molecular function.

The GO terms for up-regulated genes encompassed extracellular matrix organization, extracellular structure organization, cell-substrate adhesion, regulation of cell-substrate adhesion (e.g., *POSTN*, *SMOC2*, *COL1A1*, *CCDC80*, *FBLN1*, *ECM2*, *COL8A1*, *COL16A1*, and *ABI3BP*) and connective tissue development (*COL14A1*, *WNT9A*, *COL12A1*, and *PDGFD*), ossification signaling pathway, cellular response to transforming growth factor beta stimulus signaling pathway, and transmembrane receptor protein serine/threonine kinase signaling pathway (*ASPEN*, *COL1A2*, *LTBP3*, and *SFRP1*) (Figure 3). Most of the down-regulated genes were involved in the acute inflammatory response, neutrophil activation (e.g. *SERPINA3*, *FCER1G*, *C3AR1*, and *S100A8*), cellular modified amino acid metabolic processes (e.g., *PLA2G2A*, *MGST1*, *CHAC2*, *HOGA1*, *CHDH*, and *GNMT*), regulation of the inflammatory response (e.g., *VSIG4*, *IL1RL1*, *TLR2*, and *FCER1G*), and acute-phase response (e.g., *SERPINA3*, *CD163*, *F8*, and *EDNRB*) (Figure 4 and Figure 5).

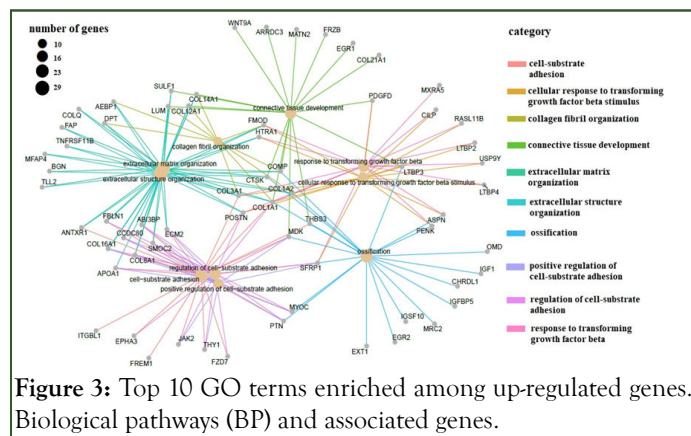


Figure 3: Top 10 GO terms enriched among up-regulated genes. Biological pathways (BP) and associated genes.

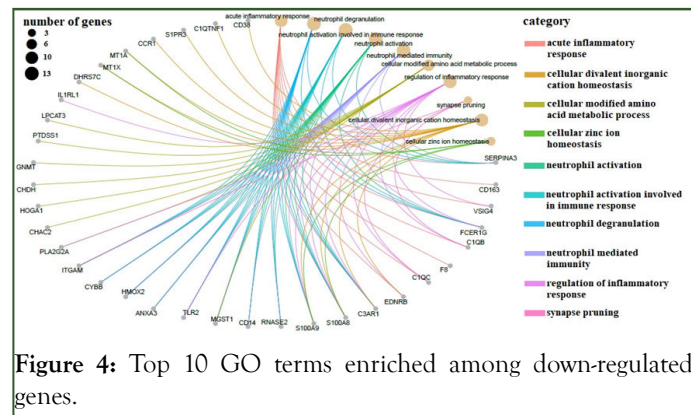


Figure 4: Top 10 GO terms enriched among down-regulated genes.

KEGG enrichment analysis showed that eight pathways had up-regulated genes and two pathways had down-regulated genes ($p < 0.05$). The pathways are shown in Figure 5.

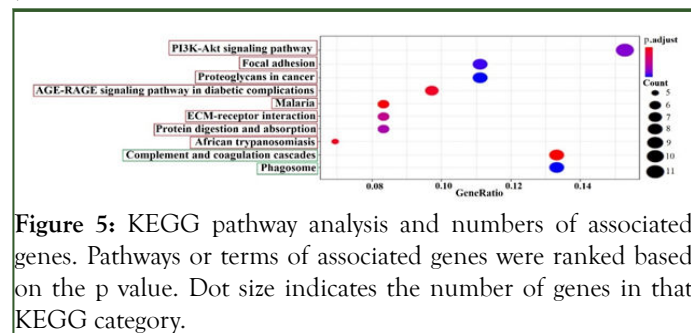


Figure 5: KEGG pathway analysis and numbers of associated genes. Pathways or terms of associated genes were ranked based on the p value. Dot size indicates the number of genes in that KEGG category.

Prediction of the miRNA-mRNA network

The up-regulated miRNA target gene regulatory network comprised 8292 genes, 45 up-regulated miRNAs, and 21,151 edges. The down-regulated miRNA-target gene regulatory network included 8075 genes, 46 down-regulated miRNAs, and 25,577 edges. Then, the sub-network for potential genes in KEGG was identified, which clearly showed the involvement of several miRNAs in potential gene regulation. We selected

leading miRNAs and potential genes *via* the involvement of many candidates in the miRNA-mRNA network. In the sub-network, 5 up-regulated and 23 down-regulated miRNAs were linked to potential genes. Several leading miRNAs showed associations with multiple genes. For instance, miR-9-5p (log2FC 1.78) targets *CCND1*, *IGF1*, and *COL12A1*; other miRNAs were linked to *IGF1*, *CCND1*, *WNT9A*, *F2R*, and *COL1A1* (Figure 6).

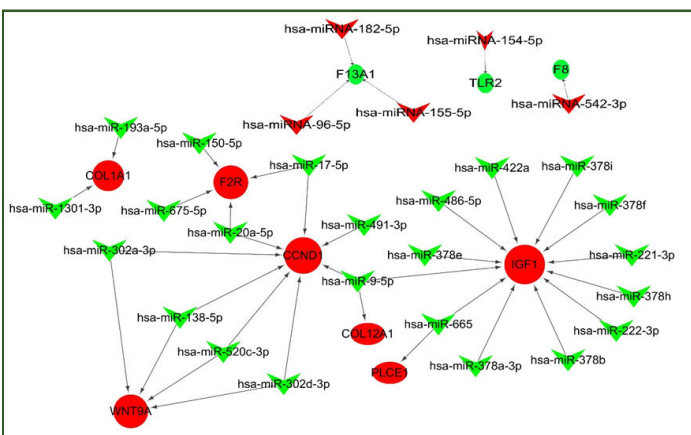


Figure 6: MiRNA-MRNA network. V, main miRNAs; symbol size, association strength; ellipses, potential genes; red, upregulated; green, downregulated.

The *COL1A1*, *IGF1*, and *CCND1* genes participated in major signaling pathways (Figure 7).

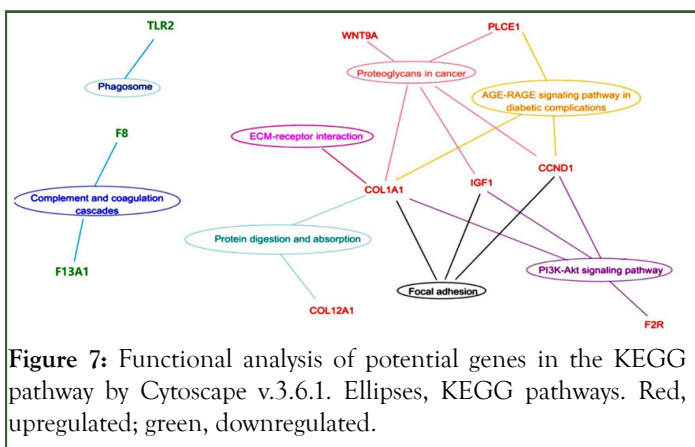


Figure 7: Functional analysis of potential genes in the KEGG pathway by Cytoscape v.3.6.1. Ellipses, KEGG pathways. Red, upregulated; green, downregulated.

Table 6: Top 3 GO enrichment analysis for modules.

Module	GO ID-Description	Count	P value	Genes in test set
Module 1	9611-response to wounding	8/20	3.35E-07	<i>CIQB</i> <i>CCR1</i> <i>C3AR1</i> <i>F13A1</i> <i>VSIG4</i> <i>FMOD</i> <i>S100A9</i> <i>CIQC</i>
	2682-regulation of immune system process	7/20	1.06E-06	<i>CIQB</i> <i>FAP</i> <i>C3AR1</i> <i>VSIG4</i> <i>THBS4</i> <i>CIQC</i> <i>TLR2</i>
	6950-response to stress	9/20	3.15E-04	<i>CIQB</i> <i>CCR1</i> <i>C3AR1</i> <i>F13A1</i> <i>VSIG4</i> <i>FMOD</i> <i>S100A9</i> <i>CIQC</i> <i>TLR2</i>
Module 2	7155-Cell adhesion	07/12	4.63E-07	<i>COMP</i> <i>COL16A1</i> <i>COL14A1</i> <i>COL12A1</i> <i>COL21A1</i> <i>COL8A1</i> <i>CTGF</i>

The PPI network encompassed 274 nodes corresponding to 274 genes with 1520 connecting edges (Figure 8A). Module 1 (confidence score 6.105) comprised 20 nodes and 58 connecting edges (Figure 8B). Module 2 (score 6.182) consisted of 12 nodes and 34 connecting edges (Figure 8C). Module 3 (score 4.667) comprised 10 nodes and 21 connecting edges (Figure 8D). Module 4 (score 3.6) consisted of six nodes and nine connecting edges (Figure 8E). These modules represent molecular complexes in the PPI networks and enhance the functional annotation accuracy and, thereby, increase reliability. Important subnets and genes of interest were selected (Table 6). The relationships between genes and the functional annotations of the modular genes warrant further investigation.

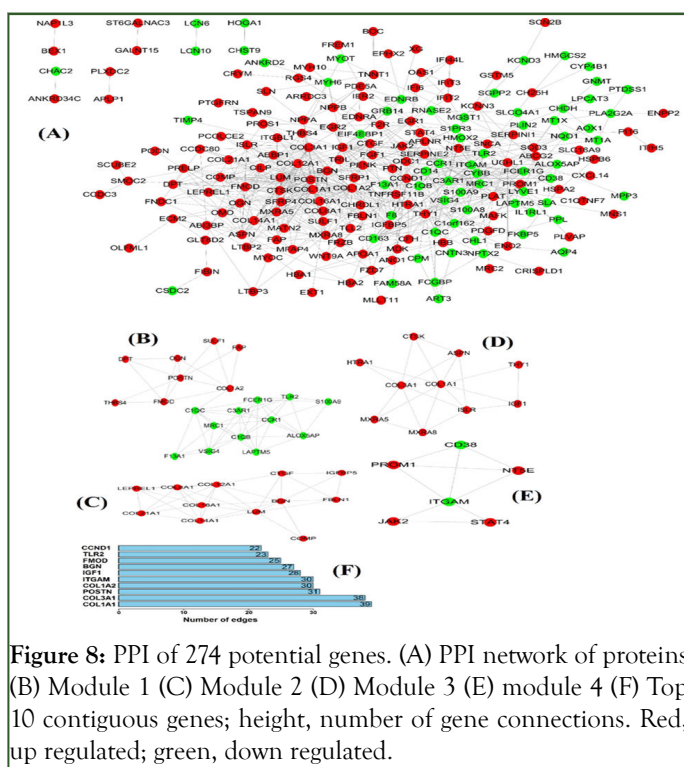
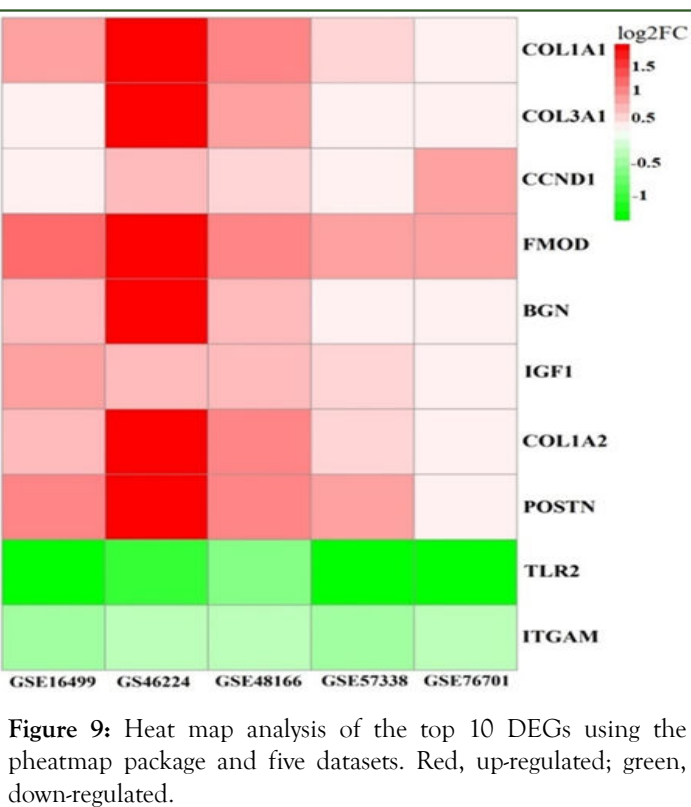


Figure 8: PPI of 274 potential genes. (A) PPI network of proteins (B) Module 1 (C) Module 2 (D) Module 3 (E) module 4 (F) Top 10 contiguous genes; height, number of gene connections. Red, up regulated; green, down regulated.

	22610-biological adhesion	07/12	4.67E-07	COMP COL14A1 COL21A1	COL16A1 COL12A1 COL8A1 CTGF
	30198-extracellular matrix organization	04/12	1.20E-06	COL14A1	LUM COL12A1 CTGF
Module 3	7275-multicellular organismal development	06-Oct	1.52E-03	COL1A1 THY1	COL3A1 IGF1 CTSC ASN
	48856-anatomical structure development	06-Oct	8.08E-04	COL1A1 THY1	COL3A1 IGF1 CTSC ASN
	48519-negative regulation of biological process	06-Oct	1.7053-4	COL1A1 THY1	COL3A1 IGF1 HTRA1 ASPN
Module 4	7166-cell surface receptor linked signaling pathway	03-Jun	1.12E-02	ITGAM	STAT4 JAK2
	10942-positive regulation of cell death	02-Jun	1.36E-02	CD38	JAK2
	6928-cellular component movement	02-Jun	1.50E-02	ITGAM	JAK2

The higher the number of connecting edges, the greater the importance of the position in the network. These genes are potential targets of miRNAs in ICM. The top ten potential genes from the PPI network with the highest degree were subjected to heat map analysis (Figure 9).



DISCUSSION

We found 274 mRNAs and 91 miRNAs that were significantly differentially expressed in ICM compared with normal controls. Differentially expressed miRNAs were mapped to their target genes and the interaction of gene nodes, such as *TLR2*, *F8*, *F13A1*, *F2R*, *CCND1*, *COL12A1*, *WNT9A*, *IGF1*, *COL1A1* and *PLCE1* were constructed. Of these *COL1A1*, *CCND1* and *IGF1* were identified as high-level central nodes, which participate in several different cellular signaling pathways.

PPI analysis suggested that *COL1A1* and *IGF1* were the most influential factors, a finding supported by the miRNA-mRNA network analysis. We thus hypothesize that these master genes are part of a gene network that is altered in ICM.

Cardiac regeneration is characterized by collagen deposition in the extracellular matrix. However, excessive deposition of collagen may cause myocardial fibrosis. *COL1A1* is a potential biomarker of HF progression. According to Huang et al., up-regulated mRNA levels of *COL1A1*, *COL8A1* and *COL3A1* were related to extracellular matrix (ECM), cell adhesion, collagen, and growth factor binding in the hearts of ICM patients. Up-regulation of *CCND1*, by contrast, is implicated in left ventricular remodeling. Alimadadi, et al. identified that *CCND1* was involved in failure of heart and/or arrhythmia, contributing to HF related cardiac disorders. In study explored molecular mechanisms, Yang, et al. showed that the circCHFR/miR-370/FOXO1/CCND1/Cyclin D1 axis provides a profound understanding of the vascular smooth muscle proliferation and migration. Li, et al. showed that up-regulation of *CCND1* is important in the development of ICM, which is consistent with our results. Concerning insulin-like growth factor 1 (*IGF1*), there is a relationship between the GH/*IGF1* axis and the cardiovascular system. The GH/*IGF1* axis regulates cardiac

growth, myocardial contractility, and the influence of the vascular system. IGF1 is involved in the development of ICM *via* its atherosclerotic effect. IGF1 receptor activation reduced ischemia/reperfusion-induced apoptosis by activating the intracellular phosphoinositide 3-kinase/protein kinase B (PI3K/Akt) signaling pathway which promotes cell survival and protects organs against ischemia/reperfusion damage. Akt phosphorylation is a downstream target of PI3K and therefore, an important intermediary of cell survival. The activation of PI3K by IGF1 induces Akt phosphorylation and activation, which reduces Reactive Oxygen Species (ROS) levels and myocardial apoptosis, thereby improving left ventricular function. However, overexpression of cardiac PI3K α or its upstream receptor IGF1 leads to myocardial enlargement and hypertrophy. Taken together, our findings suggest that *COL1A1*, *CCND1* and *IGF1* are essential in the development of ICM.

These genes and their signaling networks are involved in multiple physical and pathological processes including malaria and African trypanosomiasis, PI3K-Akt signaling, focal adhesion, protein digestion and absorption, complement and coagulation cascades, ECM-receptor interactions, and diabetic complications. Advanced glycation end products and their receptors (AGEs/RAGE), which are implicated in diabetic complications such as diabetic cardiomyopathy, were linked to ICM, implying a role in the pathogenesis of ICM. This finding is in agreement with a report that long-lived proteins such as collagen in the basement membrane are vulnerable to AGE cross-linking, leading to vascular hyper-permeability and stiffness, impaired ECM architecture, disrupted tissue homeostasis and myocardial remodeling. AGEs/RAGE may activate multiple intracellular signaling pathways including the protein kinase C (PKC), tyrosine phosphorylation of JAK-STAT, PI3K-Akt, MAPK (mitogen-activated protein kinase), and calcium signaling pathways. By activating the MAPK and PI3K-Akt signaling pathways, NADPH increases the production of ROS, activates caspase-3, and degrades nuclear DNA, leading to apoptosis. Furthermore, at high ROS levels, AGEs/RAGE increases the transcription of NF- κ B, TGF- β , Nox-1, and transcription factor activator protein-1(AP-1), further upregulating the expression of cytokines (e.g., TNF, IGF1, IFN- γ) and adhesion molecules (e.g., ICAM-1 and VCAM-1), disrupting cell function. Collectively, these findings show that AGEs/RAGE are crucial in the development of ICM.

miRNA-mRNA network analyses implicated multiple miRNAs in the regulation of potential genes and signaling pathways. Indeed, the down-regulation of miR-9-5p following ischemic injury may be related to ERMP1-mediated ER stress. miR-9-5p mediates hypoxic injury in cardiomyoblasts and its suppression prevents cardiac remodeling after acute myocardial infarction. Serum miR-9-5p is a potential diagnostic biomarker for carotid artery stenosis, and miR-9-5p expression is associated with vascular events. The serum miR-9 level was significantly higher in acute ischemic stroke patients. In an *in vivo* mouse model, an inhibitor of miR-9-5p ameliorated ischemic stroke. MiR-96 promoted myocardial hypertrophy including proliferation and elongation of cardiac muscle cells, resulting in cardiomegaly. Castellán, et al., reported that miR-96 regulates neovascularization following myocardial infarction and miR-

regulated genes for cardiovascular disease. Moreover, miR-96 is a putative therapeutic target in myocardial infarction. Ding, et al. showed that the serum miR-96-5p level in patients with acute myocardial infarction associated with coronary artery disease was lower than in healthy controls, implicating miR-96-5p in acute myocardial infarction.

We analyzed publicly available gene expression datasets of ischemic cardiomyopathy to identify differentially expressed miRNAs and construct a miRNA-mRNA-protein regulatory network. However, evaluating the roles of miRNAs in ICM using existing tools and databases is problematic; therefore, the results are speculative and need to be confirmed.

CONCLUSION

We evaluated the miRNA-mRNA expression profiles and related signaling pathways in ICM. Totals of 274 mRNAs and 91 miRNAs were significantly differentially expressed in ICM. Some DEGs (e.g., *COL1A1*, *IGF1*, and *CCND1*) were involved in different signaling pathways. MiR-9-5p regulates the expression regulation of genes implicated in ICM progression. Further *in vitro* studies are needed to confirm the function of the potential genes and their regulatory networks and to identify potential therapeutic targets for ICM.

CONFLICT OF INTEREST

The authors declare that they have no conflict of interests.

ONSENT FOR PUBLICATION

Not applicable.

AVAILABILITY OF DATA AND MATERIAL

All relevant data supporting the findings of this study are available within the article.

FUNDING

The study was supported by the National Natural Science Foundation of China (grant no. 81660241, 81860205).

ETHICS STATEMENT

GEO belong to public datasets. The contributors to the database have obtained ethical approval. Thus, our research has no ethical issues.

AUTHORS' CONTRIBUTION

PSD analyzed and interpreted data, and drafted the manuscript. JHP validated data and results. TLT, and CMTT helped in data collection. SLP designed the study and revised the manuscript. All authors read and approved the final manuscript.

REFERENCES

1. Felker GM, Shaw LK, O'Connor CM. A standardized definition of ischemic cardiomyopathy for use in clinical research. *J Am Coll Cardiol*. 2002;39(2):210-218.
2. Cabac-Pogorevici I, Muk B, Rustamova Y, Kalogeropoulos A, Tzeis S, Vardas P. Ischaemic cardiomyopathy. Pathophysiological insights, diagnostic management and the roles of revascularisation and device treatment. Gaps and dilemmas in the era of advanced technology. *Eur J Heart Fail*. 2020;22(5):789-799.
3. Briceno N, Schuster A, Lumley M, Perera D. Ischaemic cardiomyopathy: Pathophysiology, assessment and the role of revascularisation. *Heart*. 2016;102(5):397-406.
4. Nehra S, Gumina RJ, Bansal SS. Immune cell dilemma in ischemic cardiomyopathy: To heal or not to heal. *Curr Opin Physiol*. 2021;19:39-46.
5. Frank A, Bonney M, Bonney S, Weitzel L, Koepfen M, Eckle T. Myocardial ischemia reperfusion injury: From basic science to clinical bedside. *Semin Cardiothorac Vasc Anesth*. 2012;16(3):123-132.
6. Broughton KM, Wang BJ, Firouzi F, Khalafalla F, Dimmeler S, Fernandez-Aviles F, et al. Mechanisms of cardiac repair and regeneration. *Circ Res*. 2018;122(8):1151-1163.
7. Kruska M, El-Battrawy I, Behnes M, Borggrefe M, Akin I. Biomarkers in cardiomyopathies and prediction of sudden cardiac death. *Curr Pharm Biotechnol*. 2017;18(6):472-481.
8. Lu YW, Wang DZ. Non-coding RNA in ischemic and non-ischemic cardiomyopathy. *Curr Cardiol Rep*. 2018;20(11):115.
9. Nair N, Gongora E. MicroRNAs as therapeutic targets in cardiomyopathies: Myth or reality? *Biomol Concepts*. 2014;5:439-448.
10. Satoh M, Minami Y, Takahashi Y, Tabuchi T, Nakamura M. Expression of microRNA-208 is associated with adverse clinical outcomes in human dilated cardiomyopathy. *J Card Fail*. 2010;16(5):406-410.
11. Yang KC, Yamada KA, Patel AY, Topkara VK, George I, Cheema FH, et al. Deep RNA sequencing reveals dynamic regulation of myocardial noncoding RNAs in failing human heart and remodeling with mechanical circulatory support. *Circulation*. 2014;129:1009-1021.
12. Liu Y, Morley M, Brandimarto J, Hannenhalli S, Hu Y, Ashley EA, T, et al. RNA seq identifies novel myocardial gene expression signatures of heart failure. *Genomics*. 2015;105(2):83-89.
13. Kim EH, Galchev VI, Kim JY, Misek SA, Stevenson TK, Campbell MD, et al. Differential protein expression and basal lamina remodeling in human heart failure. *Proteomics Clin Appl*. 2016;10(5):585-596.
14. Ritchie ME, Phipson B, Wu D, Hu Y, Law CW, Shi W, et al. Limma powers differential expression analyses for rna-sequencing and microarray studies. *Nucleic Acids Res*. 2015;43(7):e47.
15. Kolde R, Laur S, Adler P, Vilo J. Robust rank aggregation for gene list integration and meta-analysis. *Bioinformatics*. 2012;28(4):573-580.
16. Yu G, Wang LG, Han Y, He QY. ClusterProfiler: An R package for comparing biological themes among gene clusters. *Omi A J Integ Biol*. 2012;16(5):284-287.
17. Kohl M, Wiese S, Warscheid B. Cytoscape: software for visualization and analysis of biological networks. *Methods Mol Biol*. 2011;696:291-303.
18. Szklarczyk D, Franceschini A, Wyder S, Forslund K, Heller D, Huerta-Cepas J, et al. STRING v10: Protein-protein interaction networks, integrated over the tree of life. *Nucleic Acids Res*. 2015;43:D447-52.
19. Bader GD, Hogue CW. An automated method for finding molecular complexes in large protein interaction networks. *BMC Bioinformatics*. 2003;4:2.
20. Maere S, Heymans K, Kuiper M. BiNGO: A cytoscape plugin to assess overrepresentation of gene ontology categories in biological networks. *Bioinformatics*. 2005;21(16):3448-9.
21. Tsoutsman T, Wang X, Garchow K, Riser B, Twigg S, Semsarian C. CCN2 plays a key role in extracellular matrix gene expression in severe hypertrophic cardiomyopathy and heart failure. *J Mol Cell Cardiol*. 2013;62:164-78.
22. Zhao J, Lv T, Quan J, Zhao W, Song J, Li Z, et al. Identification of target genes in cardiomyopathy with fibrosis and cardiac remodeling. *J Biomed Sci*. 2018;25(1):63.